

Accepted Manuscript

Comparison of multiple linear regression and group method of data handling models for predicting sunset yellow dye removal onto activated carbon from oak tree wood

Abdol Mohammad Ghaedi, Mohammad Mehdi Baneshi, Azam Vafaei, Alireza Rayegan Shirazi Nejad, Inderjeet Tyagi, Nitish Kumar, E. Galunin, Alexey G. Tkachev, Shilpi Agarwal, Vinod Kumar Gupta



PII: S2352-1864(18)30109-3
DOI: <https://doi.org/10.1016/j.eti.2018.06.006>
Reference: ETI 245

To appear in: *Environmental Technology & Innovation*

Received date: 9 March 2018
Revised date: 11 May 2018
Accepted date: 3 June 2018

Please cite this article as: Ghaedi A.M., Baneshi M.M., Vafaei A., Nejad A.R.S., Tyagi I., Kumar N., Galunin E., Tkachev A.G., Agarwal S., Gupta V.K., Comparison of multiple linear regression and group method of data handling models for predicting sunset yellow dye removal onto activated carbon from oak tree wood. *Environmental Technology & Innovation* (2018), <https://doi.org/10.1016/j.eti.2018.06.006>

This is a PDF file of an unedited manuscript that has been accepted for publication. As a service to our customers we are providing this early version of the manuscript. The manuscript will undergo copyediting, typesetting, and review of the resulting proof before it is published in its final form. Please note that during the production process errors may be discovered which could affect the content, and all legal disclaimers that apply to the journal pertain.

1 **Comparison of multiple linear regression and group method of data handling models for**
2 **predicting sunset yellow dye removal onto activated carbon from oak tree wood**

3 Abdol Mohammad Ghaedi¹, Mohammad Mehdi Baneshi^{2,*}, Azam Vafaei¹, Alireza Rayegan
4 Shirazi Nejad², Inderjeet Tyagi³, Nitish Kumar³, E. Galunin⁴, Alexey G. Tkachev⁴, Shilpi
5 Agarwal⁵, Vinod Kumar Gupta^{5,6*}

6 ¹Department of Chemistry, Gachsaran Branch, Islamic Azad University, P.O. Box 75818-63876,
7 Gachsaran, Iran

8 ²Social Determinants of Health Research Center, Yasuj University of Medical Sciences, Yasuj,
9 Iran

10 ³CSIR-Central Building Research Institute, Roorkee-247667, India

11 ⁴Tambov State Technical University, 106, Sovetskaya Str., Tambov, 392000, Russia

12 ⁵Department of Applied Chemistry, University of Johannesburg, Johannesburg, South Africa

13 ⁶Department of Biological Sciences, King Abdulaziz University, Jeddah 21589, Saudi Arabia

14
15
16
17
18
19
20
21
22
23 **Corresponding author e-mail:** mmbaneshi@yahoo.com; vinodfcy@gmail.com

1 Abstract

2 Activated carbon from oak tree is used as adsorbent for the removal of noxious anionic dye
3 sunset yellow. The prepared adsorbent is characterized using X-ray diffraction, Scanning
4 Electron microscopy equipped with Energy-Dispersive X-ray spectroscopy and Fourier
5 transform infrared spectroscopy. In addition to this, parameters like initial concentration,
6 adsorbent dosage, contact time, pH, and particle size on the uptake of SY dye from wastewater is
7 well investigated and optimized. For maximum adsorption, the initial concentration of 10 mg/L;
8 adsorbent dose of 0.25 g; pH =1; contact time= 35 min and particle size=150-250 μm is found to
9 be optimal value. The adsorption isotherm data at different adsorbent dosage of 0.05- 0.25 g is in
10 agreement with the Langmuir isotherm having $Q_{\text{max}} = 5.8377\text{-}30.1205$ mg/g. On the other
11 hand, models like, Group Method of Data Handling and multiple linear regression were used to
12 forecast of the removal efficiency of noxious anionic dye sunset yellow and from results, it is
13 specified that the GMDH model possess a high performance than MLR model for forecasting
14 removal percentage of SY dye. Hence, activated carbon from oak tree can be efficiently used as
15 adsorbent for the removal of SY dye from wastewater.

16 **Keywords:** Adsorption, anionic dye SY, Adsorption kinetics, Isotherms, Modelling

17

18

19

20

21

22

23

1 **1. Introduction**

2 Groundwater and surface water has been exploited due to several noxious impurities and
3 among all chemical dyes is one of the most detrimental impurity that possess serious
4 environmental side effect on human being and marine life (Garg et al., 2003; Tanzifi et al., 2018;
5 Yao et al., 2018 Gupta et al., 2011b; Gupta et al., 2013a). Synthetic dyes and pigments are
6 widely utilized as colorants in different industrial processes including the pharmaceutical, textile,
7 leather, paper, gasoline, food industries etc. and a huge amount of unused synthetic dyes is being
8 released in water streams by various industries worldwide annually. Dyes being colored in nature
9 is visible even at very low concentration and its resistive nature also decreases the sunlight
10 penetration in water. Therefore, their release into the environment presents a major source of
11 contamination (Gupta et al., 2013b; Gupta et al., 2014; Tian et al., 2018). Dyes molecules are
12 normally produced from the aromatic structure and their degradation products are toxic or even
13 carcinogenic and mutagenic. In addition to this, it leads to increased biological oxygen demand
14 (BOD) and chemical oxygen demand (COD) levels of aquatic resources (Crini, 2006; Nekouei et
15 al., 2017). Thus, it is the need of today to eliminate the toxic dyes from effluents of industries,
16 before it is released into the environment.

17 Several technologies for instance flocculation–coagulation (Szygula et al., 2009; Wang et al.,
18 2012), photodegradation (Gupta et al., 2011c; Smirnova et al., 2015; Tadjarodi et al., 2013),
19 biodegradation (Li et al., 2004), membrane separation (Bouazizi et al., 2017; Chen et al., 2017;
20 Ruan et al., 2016; Saravan et al., 2013; 2015; Tahri et al., 2016), aerobic or anaerobic treatment
21 (Fernando et al., 2013), electrochemical (Aquino et al., 2010; Riera-Torres and Gutiérrez, 2010),
22 and oxidizing agents (Ghoneim et al., 2011) have been used worldwide for the removal of
23 noxious dyes from wastewater. In spite of the growth of different techniques for treatment of dye

1 effluent, but still there are some specific challenges, for example effective, rapid and economic
2 for treatment of water and wastewater at a commercial level are going on. Among these methods
3 for water treatments, the adsorption technique by solid adsorbents is one of the most efficient
4 approaches for the uptake of dyes from industrial wastewater (Gupta et al., 2011a). The key
5 advantage of this technology is that it is scalable and large volume of effluents can be passed in a
6 single run, which lead to high quality of treated wastewaters without the formation of harmful
7 materials (Gupta et al., 2010b). This technique currently can widely be used to remove or
8 minimize diverse kinds of organic and inorganic contaminants from the aqueous media (Jain et
9 al., 2003). One of the best and effective adsorbents, which are the most extensively employed for
10 the treatment of wastewaters containing dyes, is activated carbon (Auta and Hameed, 2011; Li et
11 al., 2011; Martins and Nunes, 2015) which due to its large surface area and high porosity lead to
12 high adsorption capacity. However, two factors i.e. expensive and low regeneration rate of the
13 commercial activated carbon restrict their usage (Crini, 2006). A rising interest has recently been
14 observed in the use of alternative low cost non-conventional adsorbents including agricultural
15 waste, industrial waste, etc. for the adsorption dye from wastewater (Malik, 2003; Mall et al.,
16 2005; Prakash Kumar et al., 2005). Hence, the studies in order to obtain more efficient and
17 economic adsorbents with the higher adsorption capacity and better reusable are continuing.

18 Nowadays, artificial intelligence (AI) approaches for instance artificial neural networks
19 (ANNs), random forest (RF), adaptive neuro-fuzzy inference system (ANFIS) and support vector
20 regression (SVR) have broadly utilized for modeling of adsorption processes, which these
21 models can be generated more accurate outcomes than conventional techniques. Group method
22 of data handling (GMDH) neural network is one sub-model of ANNs, which has been widely
23 and successfully used in different fields of engineering and science. The researchers showed that

1 GMDH tool could be utilized as a successful technique in the modeling of various processes
2 (Abdolrahimi et al., 2014; Atashrouz et al., 2014; Najafzadeh and Azamathulla, 2012). Recently,
3 Yousefi and Razavi used the GMDH network to estimate the amounts of glucose release from
4 native and modified wheat starch gels during digestion under simulated gastrointestinal
5 conditions (Yousefi and Razavi, 2017). Varamesh et al. (Varamesh et al., 2017) developed the
6 GMDH as a predictive modeling method for estimation of the critical properties of pure chemical
7 compounds. Dargahi-Zarandi et al. (Dargahi-Zarandi et al., 2017) utilized GMDH as modeling
8 technique for forecasting the viscosity of pure hydrocarbon and gas mixtures including heavy
9 components and impurities for instance nitrogen, carbon dioxide and helium. Barzegar et al.
10 (Barzegar et al., 2017) developed a hybrid wavelet-GMDH model for prediction of groundwater
11 level fluctuations.

12 There were no reports on the use of the GMDH model for prediction of the adsorption
13 process. This led us to use GMDH for forecasting the uptake of SY onto AC prepared from oak
14 tree wood as cost-effective adsorbent. The produced adsorbent was considered by XRD, SEM-
15 EDX and FT-IR spectroscopy techniques. The uptake efficacy of AC was considered under the
16 important variables including particle size, contact time, concentration of dye, adsorbent dosage
17 and pH of solution. Furthermore, the kinetics and isotherm of the adsorption process was
18 considered.

19 **2. Materials and methods**

20 **2.1. Materials and instruments**

21 All chemicals i.e. SY dye (Molecular Structure is shown in Fig.1a), FeCl₃, HCl, NaCl and
22 NaOH were supplied from Merck (Darmstadt, Germany). The dye concentration of the solution
23 is determined using a Perkin Elmer UV-Vis spectrophotometer (Lambda 25, USA) and the pH

1 of the solution is measured using a Metrohm 686 pH meter (Herisau, Switzerland). A Bruker
2 AXS powder X-ray diffractometer (D8 advance, Bruker, Germany) was used to obtain the X-ray
3 diffraction (XRD). A scanning electron microscope (SEM, VEGA3 TESCAN model) equipped
4 with energy dispersive spectroscopy (EDS) was used to consider the morphology and elemental
5 composition of the prepared AC. Fourier transform infrared spectroscopy (FTIR) was achieved
6 by a Perkin Elmer Fourier transform infrared spectrometer (spectrum 65, USA).

7 **2.2. Preparation of AC**

8 Oak tree trunk timbers (OT) were employed as a precursor to prepare the activated
9 carbon. In order to eliminate the foreign materials, distilled water is used for washing, which is
10 later on dried at 120 °C for 12 h and cut into smaller pieces of about 2–3 mm. The materials were
11 mixed with 15 % FeCl₃ solution (ratio of 1g: 10mL), and soaked at room temperature for 24 h.
12 Then, the extra of FeCl₃ solution was decanted and modified OT pieces were then dried at 110
13 °C for 24 h. The treated TO pieces were exposed for carbonization for 1 h at 550 °C under
14 vacuum using a muffle furnace. It is later on cooled to room temperature and then soaked in 0.1
15 mol/L hydrochloric solution acid (ratio of 1g: 10mL) for chemical activation of the activated
16 carbon at room temperature for 24 h and then washed with distilled water several times, the
17 obtained washed product is then finally dried at 120 °C. These ACs were sieved to acquire the
18 required particle size to study adsorption.

19 **2.3. Adsorption experiments**

20 The dye stock solution in the concentration of 1000 mg/L was used to prepare the dye
21 solutions at specified concentrations using distilled water. The NaOH and HCl solutions were
22 applied for adjusting the dye solutions pH. Each experimental run was performed in 100 mL
23 Pyrex glass beaker including 50 mL of dye solutions with required concentration, quantity of

1 adsorbent, pH, contact time and particle size at room temperature. At the end of each
 2 experimental run, the solutions were filtered with Whatmann filter paper and the dye
 3 concentration was determined using the collected supernatant. The following equations were
 4 used to calculate the percent of removal (R%) and capacity of uptake (q), respectively.

$$5 \quad R \% = \frac{(C_0 - C_t)}{C_0} \times 100 \quad (1)$$

$$6 \quad q_t = \frac{(C_0 - C_t)V}{W} \quad (2)$$

7 where C_0 shows the dye initial concentration (mg/L), C_t represents the time t the dye
 8 concentration (mg/L), V indicates the solution volume (L), W displays the adsorbent weight (g)
 9 and q_t shows the time t uptake capacity of adsorbent (mg/g).

10 **2.4. Group method of data handling (GMDH)**

11 The GMDH (Fig. 1b) is a heuristic self-organizing principle-based learning machine in which
 12 a quadratic polynomial function was used to obtain each layer. Volterra–Kolmogorov–Gabor
 13 (VKG) polynomial can evaluate the relation between the input variables and the output variable.
 14 Ivakhnekoin as shown in the following equation has firstly suggested the general polynomial
 15 function of GMDH model (Ivakhnenko, 1968).

$$16 \quad \hat{y} = a_0 + \sum_{i=1}^n a_i x_i + \sum_{i=1}^n \sum_{j=1}^n a_{ij} x_i x_j + \sum_{i=1}^n \sum_{j=1}^n \sum_{k=1}^n a_{ijk} x_i x_j x_k + \dots$$

$$17 \quad (3)$$

18 The simplified equation to a quadratic polynomial containing of only two variables can be
 19 written as:

$$20 \quad \hat{y} = a_0 + a_1 x_i + a_2 x_j + a_3 x_{ij} + a_4 x_i^2 + a_5 x_j^2$$

$$21 \quad (4)$$

22 where \hat{y} , a and x indicate the anticipated output, the coefficients of polynomial set by algorithm
 23 and the input variables, respectively. The main objective in the GMDH model was obtaining a

1 function that is expected to output this function close to the experimental outputs. Therefore, to
 2 obtain the GMDH structure objective function should be minimized, which it can be described
 3 as:

$$4 \quad e = \sum_{i=1}^n (\hat{y}_i - y_i)^2 \quad (5)$$

5 where y_i represents the experimental data. Minimization of Eq. (5) can be employed to calculate
 6 the values of the coefficients of polynomial (a). These parameters can be computed from
 7 multiple regression using the least squares method, which can be achieved by solving the
 8 following matrix:

$$9 \quad A = Y^T Y \quad (6)$$

$$10 \quad Y = (1 \quad x_i \quad x_j \quad x_i x_j \quad x_i^2 \quad x_j^2) \quad (7)$$

$$11 \quad X = (a_0 \quad a_1 \quad a_2 \quad a_3 \quad a_4 \quad a_5) \quad (8)$$

12

$$13 \quad A = \begin{bmatrix} 1 & x_i & x_j & x_i x_j & x_i^2 & x_j^2 \\ x_i & x_i^2 & x_i x_j & x_i^2 x_j & x_i^3 & x_i x_j^2 \\ x_j & x_i x_j & x_j^2 & x_i x_j^2 & x_i^2 x_j & x_j^3 \\ x_i x_j & x_i^2 x_j & x_i x_j^2 & x_i^2 x_j^2 & x_i^3 x_j & x_i x_j^3 \\ x_i^2 & x_i^3 & x_i^2 x_j & x_i^3 x_j & x_i^4 & x_i^2 x_j^2 \\ x_j^2 & x_i x_j^2 & x_j^3 & x_i x_j^3 & x_i^2 x_j^2 & x_j^4 \end{bmatrix} \quad (9)$$

$$14 \quad b = (yY)^T \quad (10)$$

15 The equations can be written as:

$$16 \quad \sum_{i=1}^n AX = \sum_{i=1}^n b \quad (11)$$

17 2. 5. Assessment of models

18 For assessing the reliability and precision of the suggested models, mean square error
 19 (MSE) and determination coefficient (R^2) were employed.

$$20 \quad MSE = \frac{1}{n} \sum_{i=1}^n ((O_i)_{exp} - (O_i)_{prd})^2 \quad (12)$$

$$R^2 = 1 - \frac{\sum_{i=1}^n ((O_i)_{prd} - (O_i)_{exp})^2}{\sum_{i=1}^n ((O_i)_{exp} - O_m)^2} \quad (13)$$

where $(O_i)_{exp}$ shows the i th actual value, $(O_i)_{prd}$ presents the i th predicted value, and O_m indicates the mean value of $(O_i)_{exp}$.

3. Results and discussion

3.1. Characterization of adsorbent

The surface functional groups of the prepared AC is investigated using FTIR and the obtained spectrum is indicated in Fig. 1c. The produced AC revealed several major absorption peaks. The bands achieved at 2931, 2874 cm^{-1} are due to the C-H stretching, and $-\text{CH}_3$ group of alkane, while the peaks in the range of 2850-3000 cm^{-1} may be assigned to the dimer OH group of carboxylic acids. The band at 1723 cm^{-1} shows the C=O stretching. The peaks in the region 1400-1505 cm^{-1} may be assigned to the C-C stretching of aromatic groups. The bands in the range of 1000-1320 cm^{-1} are attributed to C-O stretching mode in carboxylic acids. The band at 731 cm^{-1} indicates the C-H mode out of plane.

The XRD pattern of the prepared AC is illustrated in Fig. 1d. The presence of sharp and broad peaks reveals that the AC is both crystalline and amorphous structures. The crystalline nature is about 26% while the amorphous nature is about 74%. Therefore, the XRD results show a mostly amorphous nature of the prepared AC with low crystallinity. The peaks detected in XRD patterns for the AC sample are similar to the (002), (100) and (101) planes which attributed to the graphite peaks (Rajendran et al., 2015).

The SEM micrographs of the produced AC surface illustrated the rough surface and cavities on the AC samples as depicted in Fig. 1e. These cavities on the sample surface significantly increase the surface available for dyes and metal ions uptake. A semi-quantitative study of the

1 AC can be obtained using the EDS analysis. Fig. 1f displays the results of the EDS investigation
2 for the AC samples. The AC sample indicates the carbon, oxygen and nitrogen content (%
3 atomic) as 70.57, 24.17 and 5.26, respectively.

5 **3.2. Impact of pH**

6 The solution pH is known as one of the significant factor in the adsorption process because
7 of its influences the surface charge of both adsorbent and dye molecules (Errais et al., 2011;
8 Kumar et al., 2010; Rafatullah et al., 2010). Influence of initial pH of solution on the SY dye
9 uptake with concentration of 15 mg/L, adsorbent dose of 0.2 g, particle size of 150-250 μm ,
10 stirrer speeds of 600 rpm and contact times of 35 min is well studied and the results obtained is
11 shown in Fig. 2a. reveals the uptake behavior of SY dye on adsorbent at pH values ranging from
12 1 to 10. As the figure shows, by growing the pH from 1 to 10 the dye removal significantly
13 declines to 21.97% from 83.33%. These findings indicate that our results are in agreement with
14 previous investigations (Çelekli et al., 2012; Çelekli et al., 2012; Gupta et al., 2010a). It is
15 needed to specify the zero point charge (pH_{zpc}) of adsorbent is one of the main factor to
16 recognize the mechanism of sorption. Fig. 2b shows that the pH_{zpc} of the adsorbent is found to be
17 about 3.0. The adsorbent surface could become positively charged at $\text{pH} < \text{pH}_{\text{zpc}}$, thereby a high
18 electrostatic attraction occurs between positive charges of adsorbent and negative charges of
19 anionic dyes such as SY dye. At higher pH values than pH_{zpc} , the surface of the adsorbent could
20 be negatively charged, which decrease in the percentage removal of anionic dye because of
21 electrostatic repulsion. The maximum percentage dye removal was obtained at pH 1. Hence, this
22 pH value is the optimal value for the rapid adsorption of noxious SY dye.

23 **3.3. Impact of particle size**

1 For investigating the effect of particle size on the adsorption of SY dyes, three particle sizes
2 (150–250, 250–425, and 425–850 μm) of AC in a beaker containing 50 mL of the adsorption
3 solution with 10–40 mg/L, 5–35 min, 0.05–0.25 g and 600 rpm was used. The results obtained is
4 shown in Fig. 3, which demonstrates the influence of particle size on adsorption of SY dye with
5 concentration of 10 mg/L and contact time of 35 min. The results of the effect of particle size at
6 different contact time is included in the supporting information (Fig. S1). From Fig 3 and Fig S1
7 it was observed that as the particle size increases from 150–250 to 425–850 μm with dye
8 concentration of 10 mg/L, adsorbent dosage of 0.25 g and contact time of 35 min, the removal
9 percentage decreases from 88.30 to 65.07 %. This is because of increased surface area and large
10 number of available active sites for molecules of noxious SY dye. Similar results have been
11 obtained in previous studies (Celekli et al., 2012; Gupta et al., 2010a; Mui et al., 2010).

12 **3.4. Effect of contact time**

13 Various experiments at five contact times (5, 10, 20, 30 and 35 min) under different
14 operating variables (particle size of 150–850 μm , adsorbent dosage of 0.05–0.25 g, pH 1, 600
15 rpm and dye concentration of 10–40 mg/L) were performed to assess impacts of contact time on
16 the SY dye adsorption on AC (Figs. 4 and S2). From the results obtained, it is observed that the
17 values of SY dye removal increases with contact time up to 10 mins and then remains constant
18 with further increase in contact time. The fast sorption may be attributed to the abundance of
19 functional groups on the surface of the adsorbent during beginning contact time steps.

20 **3.5. Impact of dye concentration**

21 To estimate impact of dye concentration on the removal percentage of dye, experiments
22 were performed at diverse quantity of adsorbents (0.05–0.25 g) and four dye concentrations (10–
23 40 mg/L) for three particle sizes (150–250, 250–425, and 425–850 μm). Figs. 5 and S3

1 demonstrate the variation in removal percentage values versus dye concentration for SY. Results
2 specified that the removal of SY dye significantly decreased with dye concentration. This could
3 be the result of decline in the surface area of available unoccupied sites by enhancing in
4 concentration of dye. Results also showed that value of adsorption capacity improved by
5 elevating concentration of dye. The increment in the driving force for mass transfer by
6 improving in concentration of dye could be the reason for this phenomenon. These results are in
7 agreement with the results of previous adsorption investigations (Dehghanian et al., 2015;
8 Ghaedi et al., 2014).

9 **3.6. Impact of adsorbent dosage**

10 To calculate the impact of the adsorbent amount on the uptake of SY dye, five adsorbent
11 dosage (0.05-0.25 g) were used with three particle sizes (150–850 μm) at the dye solution with
12 four SY dye concentrations (10-40 mg/L). The result of the amount of adsorbent on the removal
13 percentage of SY dye is displayed in Figs. 5 and S4. As seen from this figure, an enhancement in
14 the dosage of adsorbent from 0.05 to 0.25 g improved the removal percentage values because of
15 enhancement in active site and surface area. The same result was also obtained for the adsorption
16 of methyl orange dye on tin oxide nanoparticles loaded on AC achieved from *Pistacia atlantica*
17 wood (Ghaedi et al., 2016).

18 **3.7. Adsorption kinetics**

19 For considering the kinetic of SY dye uptake on produced adsorbent Lagergren's pseudo-
20 first-order, the pseudo-second-order, Elovich and intraparticle diffusion were employed. The
21 equation of Lagergren's pseudo-first-order is denoted as (Azizian, 2004; Lagergren, 1898),

$$22 \ln(q_e - q_t) = \ln q_e - k_1 t \quad (14)$$

1 where q_e , q_t and k_1 are the capacity of dye uptake at equilibrium (mg/g), the capacity of dye
 2 uptake at time t (mg/g), the rate constant of the first-order reaction (l/min). The pseudo-second-
 3 order can be indicated in the linear form (Ho, 2006; Ho and McKay, 1998).

$$4 \quad t/q_t = 1/(k_2 q_e^2) + (1/q_e) \cdot t \quad (15)$$

5 where k_2 represents rate constant of the second-order reaction (g/mg min). The Elovich model
 6 can be expressed by the following relation (Ho and McKay, 2002; Rudziński and Everett, 1992).

$$7 \quad q_t = \frac{1}{\beta} \ln(\alpha\beta) + \frac{1}{\beta} \ln t \quad (16)$$

8 where β is the desorption coefficient ($\text{mg g}^{-1} \text{min}^{-1}$) and α is the initial adsorption rate (g mg^{-1}
 9 min^{-2}). Finally, the simplified intra-particle diffusion model to achieve the diffusion rate
 10 coefficient may be written as below (Weber and Morris, 1963).

$$11 \quad q_t = k_i \cdot t^{0.5} + C \quad (17)$$

12 where k_i represents the rate coefficient ($\text{mg g}^{-1} \text{min}^{-0.5}$). The slope and intercept of the linear
 13 plot of q_t vs. $t^{0.5}$ can be used to find k_i and C (mg g^{-1}), respectively. The values obtained for the
 14 parameters of kinetic models in order to the removal of SY dye on AC at room temperature, pH
 15 1, 600 rpm, 40 mg/L, 150-250 μm and different adsorbent dosage have been shown in Table S2.
 16 Based on the high values of R^2 (in the range of 0.9959-0.9984) can be deduced that the pseudo-
 17 second-order kinetic is appropriate for demonstrating the SY dye uptake on AC. Three steps
 18 including pore diffusion, film diffusion and intra-particle transport determine the mechanism of
 19 the absorption process. The process overall rate is controlled using the slowest of the three steps.
 20 To find the mechanisms of SY dye uptake on AC, the intra-particle diffusion model (Eq. 17) was
 21 used which in this equation C value indicates the boundary layer thickness. Thus, it can be
 22 deduced that the pore diffusion is not the only rate-limiting step whereas the rate-controlling step
 23 is probably chemical interactions (Ahmad, 2009).

1 3.8. Adsorption isotherms

2 The equilibrium adsorption of the SY dye was performed with different adsorbent
3 amount (0.05-0.25 g) with particle size of 150- 250 μm in 50 ml solution of dye with diverse
4 concentrations from 10 - 40 mg/L for 35 minutes at pH 1. Four types of several isotherm models
5 namely Freundlich, Langmuir, Dubinin-Raduskevich (D-R) and Temkin were used to fit the
6 actual data. The isotherm parameters achieved by linear fitting were indicated in Table S3.

7 The Langmuir isotherm describes the formation of the uniform monolayer adsorption on the
8 adsorbent surface (Langmuir, 1916). The linear form of Langmuir equation can be indicated as
9 follow:

$$10 \frac{C_e}{q_e} = \frac{1}{q_m K_L} + \frac{C_e}{q_m} \quad (18)$$

11 where C_e shows concentration of adsorbate at equilibrium (mg/L), q_e is capacity of adsorption
12 at equilibrium (mg/g), q_m displays maximum capacity of monolayer coverage (mg/g) and K_L is
13 constant of Langmuir isotherm (L/mg). Equilibrium parameter or separation factor (R_L) as main
14 characteristics of the Langmuir model can be expressed as follows:

$$15 R_L = \frac{1}{1 + K_L C_0} \quad (19)$$

16 The value of R_L displays whether the nature of adsorption is favorable or unfavorable; linear if
17 $R_L=1$, favorable if $0 < R_L < 1$, unfavorable if $R_L > 1$ and irreversible if $R_L=0$. As seen from Table 1,
18 the R_L values were between 0 and 1 representing that Langmuir isotherm is favorable. From the
19 result obtained, the q_m from Langmuir Isotherm model was found to be 5.8377- 30.1205 mg/g,
20 K_L values are between 0.1453 and 0.4287 L/mg. The R^2 values were obtained to be 0.9862-
21 0.9954, demonstrating that the adsorption of SY dye on AC fitted well to the Langmuir Isotherm.

1 Freundlich isotherm has been applied for describing the adsorption onto heterogenous
 2 surfaces (Freundlich, 1906). Linearizing equation of the Freundlich isotherm can be indicated as
 3 follows:

$$4 \log q_e = \log K_F + \frac{1}{n} \log C_e \quad (20)$$

5 Where, K_F shows the capacity of adsorption (L/mg). $1/n$ represents intensity of adsorption and
 6 the distribution of the surface heterogeneity and the energy of the active sites; the partition of
 7 adsorbents between the two phases is independent of the concentration if $n=1$, normal adsorption
 8 if $\frac{1}{n} < 1$ and cooperative adsorption $\frac{1}{n} > 1$. The R^2 values of 0.8843-0.9353 indicated that
 9 Freundlich model was inadequate to explain the association of q_e with equilibrium
 10 concentrations. The values of K_F were found as 1.9315- 4.9615. The value of $1/n = 0.3884$ -
 11 0.5379 showing that the uptake of SY dye onto AC is favorable, while this model is inadequate
 12 to designate the relationship between the C_e and q_e because of the low R^2 values.

13 D-R model is usually used for discovering the adsorption mechanism based on the
 14 Gaussian energy distribution onto a heterogeneous surface (Dubinin and Radushkevich, 1947).
 15 The linear form of this model is as follows.

$$16 \ln q_e = \ln q_m - \beta \varepsilon^2 \quad (21)$$

$$17 \varepsilon = RT \ln\left(1 + \frac{1}{C_e}\right) \quad (22)$$

$$18 E = \frac{1}{\sqrt{-2\beta}} \quad (23)$$

19 where q_m (mg/g), q_e (mg/g), β (mol^2/J^2), E (J/mol) and ε are maximum uptake capacity,
 20 equilibrium adsorption capacity, activity coefficient, mean free energy of adsorption and Polanyi
 21 potential. The E -value shows the nature of adsorption to be either chemical if $8 < E < 16$ KJ/mol
 22 and physical if $E < 8$ KJ/mol. By the linear regression analysis of D-R isotherm, the values of q_m

1 were measured to 4.7684-20.5426 mg/g. The value of E parameter (0.707-1.118 KJ/mol)
2 indicating that SY dye uptake onto AC could be performed through the physical mechanism. The
3 R^2 values of D-R model were less than of Langmuir, nevertheless based on the relatively high
4 value of R^2 (0.9777-0.9869), it was deduced that the D-R model was also suitable to illustrate the
5 association of q_e with C_e .

6 The Temkin model supposes that the adsorption heat would reduce linearly and a uniform
7 distribution of binding energies was used to characterize the adsorption (Temkin and Pyzhev,
8 1940). The following relation can show this model.

$$9 \quad q_e = B \ln K_T + B \ln C_e \quad (24)$$

$$10 \quad B = \frac{RT}{b} \quad (25)$$

11 where K_T (L/g) and b (J/mol) are Temkin isotherm constant. From linear regression of Temkin
12 isotherm equation revealed in Table 1, the following values were obtained: $K_T = 1.1935$ - 4.5108
13 L/g, $B=1.2348$ - 7.2020 J/mol and $R^2=0.9537$ - 0.9842 .

14 **3.9. GMDH model**

15 In this work, the GMDH model was utilized to forecast of removal percentage of SY using
16 AC from aqueous system. Table S1 exhibits the experimental data. The actual data consist 300
17 points while 70% of these data were utilized for training and 30% for testing. The independent
18 factors for example particle size, initial concentration of dye, adsorbent dosage and contact time
19 have been designated as the inputs and the dye removal (%) has considered as the output of the
20 network. The values of these parameters with related values of R^2 and MSE were reported in
21 Table 1. To acquire the optimal construction of GMDH neural network model different
22 parameters of GMDH model for instance maximum number of layers, maximum neurons
23 number in a layer, selection pressure and train ratio were investigated. The maximum R^2 value

1 and the minimum MSE value for the testing data points were used for selection the optimal
2 construction of the GMDH model. It can be detected that the GMDH model with 100 maximum
3 layer numbers, 6 maximum neuron numbers in a layer, 0.1 selection pressure and 0.7 train ratio
4 has good performance for predicting the removal percentage of SY dye onto AC. For testing
5 points the values of R^2 and MSE were found to be 0.9702 and 3.4078 using the optimal GMDH
6 model, respectively. In addition, the actual and anticipated data were compared in Fig. 6. As
7 shown, the results of the MGDH model are in good agreement with the actual data.

8

9 **3.10. MLR model**

10 The common objective of MLR is to learn more about the association among several
11 independent parameters and a dependent parameter. The MLR equation can be written as follow
12 form.

$$13 \quad y = a + b_1x_1 + b_2x_2 + \dots + b_nx_n \quad (26)$$

14 where b_1 , b_2 and b_n are the coefficients of regression and a is a constant. The same data used in
15 the training and testing of GMDH model was used to construct and evaluate the MLR model.
16 The MLR equation to forecast removal percent is shown below.

$$17 \quad \text{Removal \%} = 45.347 + 0.222X_1 - 0.612X_2 + 0.348X_3 + 55.542X_4 \quad (27)$$

18 where X_1 , X_2 , X_3 and X_4 are particle size (mesh), initial concentration (mg/L), and adsorbent
19 dosage (g). Fig. 6 illustrates the relations between actual and forecasted values achieved from the
20 MLR model. According to this figure, the MLR results are not very close to the actual results
21 and the R^2 and MSE values were found to be 0.780 and 26.839 for testing data sets, respectively.

22 **3.11. Comparison GMDH and MLR models**

1 To compare reliable prediction of GMDH and MLR models for forecasting of removal
2 percent, the MSE, R^2 and the deviations from the actual values were calculated. Fig. 6 shows the
3 distances of the anticipated values using the models built from the experimental values. The
4 figure designated that the deviation distance (-5.0573 to +4.7495) of the forecasted values using
5 MGDH model is lower than the deviation distance of the MLR model (-10.822 to +11.739).
6 Table 4S indicates the values of R^2 and MSE for training and testing data points from both
7 GMDH and MLR models. The values of R^2 and MSE of GMDH model for training and testing
8 subsets were found to be 0.9785, 0.9702 and 2.8362, 3.4078, respectively. The R^2 and MSE
9 values of MLR model were 0.8434, 0.780 and 20.617, 26.839, respectively. Based on the MSE,
10 R^2 and the deviation interval values, it can be concluded that the GMDH model for predicting of
11 removal percent revealed the more reliable anticipations than the MLR model.

12 **4. Conclusions**

13 Biomaterial of Oak Tree is used for the preparation of AC and the prepared inexpensive
14 adsorbent is characterized using SEM, XRD and FTIR. The prepared adsorbent is 26%
15 crystalline in nature and 74 % amorphous in nature. Effective parameters were investigated and
16 optimized and it was observed that for maximum adsorption, the initial concentration of 10
17 mg/L; adsorbent dose of 0.25 g; pH =1; contact time= 35 min and particle size=150-250 μm is
18 found to be optimized. Comparison of the MLR and GMDH models showed the good
19 predictability of GMDH model for forecasting removal percent of SY dye. The optimal
20 parameters for GMDH model were found to be 100 maximum number of layers, 6 maximum
21 number of neurons in a layer, 0.1-selection pressure and 0.7 train ratio. For training points, the
22 values of R^2 of 0.9785 and MSE of 2.8362 were obtained using the optimal GMDH model. The
23 results presented that the soft computing model is a good tool for predicting adsorption process.

1 **Acknowledgments**

2 The authors would like to acknowledge the support and fund provided by the Yasuj University of
3 Medical Science (IR.YUMS.REC.1396.40). The authors would also like to acknowledge the
4 Gachsaran Branch, Islamic Azad University for the financial support of this work.

5

6

7

8

9

10 **References**

11

12 Abdolrahimi, S., et al., 2014. Prediction of partition coefficients of alkaloids in ionic liquids
13 based aqueous biphasic systems using hybrid group method of data handling (GMDH)
14 neural network. *Journal of Molecular Liquids*. 191, 79-84.

15 Ahmad, R., 2009. Studies on adsorption of crystal violet dye from aqueous solution onto
16 coniferous pinus bark powder (CPBP). *J Hazard Mater*. 171, 767-73.

17 Aquino, J. M., et al., 2010. Electrochemical degradation of the Acid Blue 62 dye on a β -PbO₂
18 anode assessed by the response surface methodology. *Journal of Applied*
19 *Electrochemistry*. 40, 1751-1757.

20 Atashrouz, S., et al., 2014. Modeling of surface tension for ionic liquids using group method of
21 data handling. *Ionics*. 21, 1595-1603.

22 Auta, M., Hameed, B. H., 2011. Optimized waste tea activated carbon for adsorption of
23 Methylene Blue and Acid Blue 29 dyes using response surface methodology. *Chemical*
24 *Engineering Journal*. 175, 233-243.

- 1 Azizian, S., 2004. Kinetic models of sorption: a theoretical analysis. *J Colloid Interface Sci.* 276,
2 47-52.
- 3 Barzegar, R., et al., 2017. Forecasting of groundwater level fluctuations using ensemble hybrid
4 multi-wavelet neural network-based models. *Sci Total Environ.* 599-600, 20-31.
- 5 Bouazizi, A., et al., 2017. Development of a new TiO₂ ultrafiltration membrane on flat ceramic
6 support made from natural bentonite and micronized phosphate and applied for dye
7 removal. *Ceramics International.* 43, 1479-1487.
- 8 Celekli, A., et al., 2012. Prediction of removal efficiency of Lanaset Red G on walnut husk using
9 artificial neural network model. *Bioresour Technol.* 103, 64-70.
- 10 Çelekli, A., et al., 2012. Sorption equilibrium, kinetic, thermodynamic, and desorption studies of
11 Reactive Red 120 on *Chara contraria*. *Chemical Engineering Journal.* 191, 228-235.
- 12 Chen, P., et al., 2017. Performance of ceramic nanofiltration membrane for desalination of dye
13 solutions containing NaCl and Na₂SO₄. *Desalination.* 404, 102-111.
- 14 Crini, G., 2006. Non-conventional low-cost adsorbents for dye removal: a review. *Bioresource*
15 *technology.* 97, 1061-1085.
- 16 Dargahi-Zarandi, A., et al., 2017. Modeling gas/vapor viscosity of hydrocarbon fluids using a
17 hybrid GMDH-type neural network system. *Journal of Molecular Liquids.* 236, 162-171.
- 18 Dehghanian, N., et al., 2015. A random forest approach for predicting the removal of Congo red
19 from aqueous solutions by adsorption onto tin sulfide nanoparticles loaded on activated
20 carbon. *Desalination and Water Treatment.* 57, 9272-9285.
- 21 Dubinin, M. M., Radushkevich, L., 1947. Equation of the characteristic curve of activated
22 charcoal. *Chem. Zentr.* 1, 875.

- 1 Errais, E., et al., 2011. Efficient anionic dye adsorption on natural untreated clay: Kinetic study
2 and thermodynamic parameters. *Desalination*. 275, 74-81.
- 3 Fernando, E., et al., 2013. Simultaneous co-metabolic decolourisation of azo dye mixtures and
4 bio-electricity generation under thermophilic (50 degrees C) and saline conditions by an
5 adapted anaerobic mixed culture in microbial fuel cells. *Bioresour Technol*. 127, 1-8.
- 6 Freundlich, H., 1906. Over the adsorption in solution. *J. Phys. Chem*. 57, 1100-1107.
- 7 Garg, V. K., et al., 2003. Dye removal from aqueous solution by adsorption on treated sawdust.
8 *Bioresource Technology*. 89, 121-124.
- 9 Ghaedi, M., et al., 2014. Random forest model for removal of bromophenol blue using activated
10 carbon obtained from *Astragalus bisulcatus* tree. *Journal of Industrial and Engineering*
11 *Chemistry*. 20, 1793-1803.
- 12 Ghaedi, M., et al., 2016. Application of least squares support vector regression and linear
13 multiple regression for modeling removal of methyl orange onto tin oxide nanoparticles
14 loaded on activated carbon and activated carbon prepared from *Pistacia atlantica* wood. *J*
15 *Colloid Interface Sci*. 461, 425-34.
- 16 Ghoneim, M. M., et al., 2011. Ghoneim, M. M., El-Desoky, H. S., & Zidan, N. M. (2011).
17 Electro-Fenton oxidation of Sunset Yellow FCF azo-dye in aqueous solutions.
18 *Desalination*. 274, 22-30.
- 19 Gupta V.K. et al., 2014 A novel magnetic Fe@Au core-shell nanoparticles anchored graphene
20 oxide recyclable nanocatalyst for the reduction of nitrophenol compounds, *Water*
21 *Research*, 2014, 48, 210-217
- 22 Gupta, V. K., et al., 2010a. Adsorptive removal of Cyanosine from wastewater using coconut
23 husks. *Journal of colloid and interface science*. 347, 309-314.

- 1 Gupta, V. K., et al., 2010b. Biosorption of nickel onto treated alga (*Oedogonium hatei*):
2 application of isotherm and kinetic models. *Journal of Colloid and Interface Science*. 342,
3 533-539.
- 4 Gupta, V. K., et al., 2011b. A comparative investigation on adsorption performances of
5 mesoporous activated carbon prepared from waste rubber tire and activated carbon for a
6 hazardous azo dye--Acid Blue 113. *J Hazard Mater*. 186, 891-901.
- 7 Gupta, V. K., et al., 2011c. Removal of the hazardous dye—tartrazine by photodegradation on
8 titanium dioxide surface. *Materials Science and Engineering: C*. 31, 1062-1067.
- 9 Gupta, V. K., et al., 2013a. Adsorptive removal of dyes from aqueous solution onto carbon
10 nanotubes: a review. *Advances in Colloid and Interface Science*. 193, 24-34.
- 11 Gupta, V. K., et al., 2013b. Adsorptive removal of dyes from aqueous solution onto carbon
12 nanotubes: a review. *Adv Colloid Interface Sci*. 193-194, 24-34.
- 13 Gupta, V., et al., 2011a. A comparative investigation on adsorption performances of mesoporous
14 activated carbon prepared from waste rubber tire and activated carbon for a hazardous
15 azo dye—Acid Blue 113. *Journal of Hazardous Materials*. 186, 891-901.
- 16 Ho, Y. S., 2006. Review of second-order models for adsorption systems. *J Hazard Mater*. 136,
17 681-9.
- 18 Ho, Y. S., McKay, G., 1998. Sorption of dye from aqueous solution by peat. *Chemical*
19 *Engineering Journal*. 70, 115-124.
- 20 Ho, Y., McKay, G., 2002. Application of kinetic models to the sorption of copper (II) on to peat.
21 *Adsorption Science & Technology*. 20, 797-815.
- 22 Ivakhnenko, A. G., 1968. The Group Method of Data of Handling; A rival of the method of
23 stochastic approximation. *Soviet Automatic Control*. 13, 43-55.

- 1 Jain, A., et al., 2003. Utilization of industrial waste products as adsorbents for the removal of
2 dyes. *Journal of hazardous materials*. 101, 31-42.
- 3 Kumar, P. S., et al., 2010. Adsorption of dye from aqueous solution by cashew nut shell: Studies
4 on equilibrium isotherm, kinetics and thermodynamics of interactions. *Desalination*. 261,
5 52-60.
- 6 Lagergren, S., 1898. Zur theorie der sogenannten adsorption geloster stoffe. *Kungliga svenska*
7 *vetenskapsakademiens. Handlingar*. 24, 1-39.
- 8 Langmuir, I., 1916. The constitution and fundamental properties of solids and liquids. Part I.
9 Solids. *Journal of the American chemical society*. 38, 2221-2295.
- 10 Li, J. G., et al., 2004. Biodegradation of Red B dye by *Bacillus* sp. OY1-2. *Environ Technol*. 25,
11 1167-76.
- 12 Li, W.-H., et al., 2011. Preparation and utilization of sludge-based activated carbon for the
13 adsorption of dyes from aqueous solutions. *Chemical Engineering Journal*. 171, 320-327.
- 14 Malik, P. K., 2003. Use of activated carbons prepared from sawdust and rice-husk for adsorption
15 of acid dyes: a case study of Acid Yellow 36. *Dyes and Pigments*. 56, 239-249.
- 16 Mall, I. D., et al., 2005. Adsorptive removal of malachite green dye from aqueous solution by
17 bagasse fly ash and activated carbon-kinetic study and equilibrium isotherm analyses.
18 *Colloids and Surfaces A: Physicochemical and Engineering Aspects*. 264, 17-28.
- 19 Martins, A., Nunes, N., 2015. Adsorption of a Textile Dye on Commercial Activated Carbon: A
20 Simple Experiment To Explore the Role of Surface Chemistry and Ionic Strength.
21 *Journal of Chemical Education*. 92, 143-147.
- 22 Mui, E. L., et al., 2010. Dye adsorption onto char from bamboo. *Journal of Hazardous Materials*.
23 177, 1001-1005.

- 1 Najafzadeh, M., Azamathulla, H. M., 2012. Group method of data handling to predict scour
2 depth around bridge piers. *Neural Computing and Applications*. 23, 2107-2112.
- 3 Nekouei, F., Nekouei, S., 2017 Cr(OH)₃-NPs-CNC hybrid nanocomposite: a sorbent for
4 adsorptive removal of methylene blue and malachite green from solutions, *Environ. Sci.*
5 *Pollut. Res.*, 24, 25291–25308.
- 6 Prakash Kumar, B. G., et al., 2005. Adsorption of Bismark Brown dye on activated carbons
7 prepared from rubberwood sawdust (*Hevea brasiliensis*) using different activation
8 methods. *J Hazard Mater*. 126, 63-70.
- 9 Rafatullah, M., et al., 2010. Adsorption of methylene blue on low-cost adsorbents: a review.
10 *Journal of hazardous materials*. 177, 70-80.
- 11 Rajendran, A. B., et al., 2015. Characterization studies of activated carbon from low cost
12 agricultural waste: *Leucaena leucocephala* seed shell. *RASAYAN Journal of Chemistry*.
13 8, 330 – 338.
- 14 Riera-Torres, M., Gutiérrez, M.-C., 2010. Colour removal of three reactive dyes by UV light
15 exposure after electrochemical treatment. *Chemical Engineering Journal*. 156, 114-120.
- 16 Ruan, H., et al., 2016. Fabrication of a MIL-53(Al) Nanocomposite Membrane and Potential
17 Application in Desalination of Dye Solutions. *Industrial & Engineering Chemistry*
18 *Research*. 55, 12099-12110.
- 19 Rudziński, W., Everett, D., 1992. Adsorption of Gases on Heterogeneous Surfaces Academic
20 Press, London. Google Scholar.
- 21 Saravan R. et al., 2013; ZnO/Ag nanocomposite: An efficient catalyst for degradation studies of
22 textile effluents under visible light, *Materials Science and Engineering C*, 33, 2235-2244.

- 1 Saravan, R., et al., 2015; ZnO/Ag/CdO nanocomposite for visible light-induced photocatalytic
2 degradation of industrial textile effluents, *Journal of Colloid and Interface Science*, 452,
3 126-133
- 4 Smirnova, N. P., et al., 2015. Photodegradation of dye acridine yellow on the surface of
5 mesoporous TiO₂, SiO₂/TiO₂ and SiO₂ films: spectroscopic and theoretical studies.
6 *Journal of Nanostructure in Chemistry*. 5, 333-346.
- 7 Szygula, A., et al., 2009. Removal of an anionic dye (Acid Blue 92) by coagulation-flocculation
8 using chitosan. *J Environ Manage.* 90, 2979-86.
- 9 Tadjarodi, A., et al., 2013. Experimental design to optimize the synthesis of CdO cauliflower-
10 like nanostructure and high performance in photodegradation of toxic azo dyes. *Materials*
11 *Research Bulletin*. 48, 935-942.
- 12 Tahri, N., et al., 2016. Preparation of an asymmetric microporous carbon membrane for
13 ultrafiltration separation: application to the treatment of industrial dyeing effluent.
14 *Desalination and Water Treatment*. 57, 23473-23488.
- 15 Tanzifi M., et al., 2018, Modelling of dye adsorption from aqueous solution on
16 polyaniline/carboxymethyl cellulose/TiO₂ nanocomposites, *J. Colloid Interface*
17 *Sci.*, 2018, 519, 154-173.
- 18 Tempkin, M., Pyzhev, V., 1940. Kinetics of ammonia synthesis on promoted iron catalyst. *Acta*
19 *Phys. Chim. USSR*. 12, 327.
- 20 Tian, W., et al., 2018 One-step synthesis of flour-derived functional nanocarbons with
21 hierarchical pores for versatile environmental applications, *Chem. Eng. J.*, 347, 432–439.
- 22 Varamesh, A., et al., 2017. Generalized models for predicting the critical properties of pure
23 chemical compounds. *Journal of Molecular Liquids*. 240, 777-793.

- 1 Wang, Y.-F., et al., 2012. Removal of acid and direct dye by epichlorohydrin–dimethylamine:
2 Flocculation performance and floc aggregation properties. *Bioresource Technology*. 113,
3 265-271.
- 4 Weber, W. J., Morris, J. C., 1963. Kinetics of adsorption on carbon from solution. *Journal of the*
5 *Sanitary Engineering Division*. 89, 31-60.
- 6 Yao, Y., et al., 2017 Synthesis of “Sea Urchin”-like Carbon Nanotubes/Porous Carbon
7 Superstructures Derived from Waste Biomass for Treatment of Various Contaminants
8 *Appl. Catal. B: Environ.*, 219, 563-571.
- 9 Yousefi, A. R., Razavi, S. M., 2017. Modeling of glucose release from native and modified
10 wheat starch gels during in vitro gastrointestinal digestion using artificial intelligence
11 methods. *Int J Biol Macromol*. 97, 752-760.

12
13
14
15
16
17
18
19
20
21
22
23

1
2
3
4
5
6
7
8
9
10
11
12
13
14
15
16
17
18
19
20
21
22
23

Figure captions:

Fig. 1. (a) molecular structures of the sunset yellow dye, (b) a schematic diagram of the used GMDH model, (c) FT-IR spectrum, (d) XRD pattern, (e) SEM image and (f) EDX analysis of the produced AC

Fig. 2. (a) Impact of pH solution on the removal of SY dye and (b) adsorbent surface charge as a function of pH

Fig. 3. Influence of particle size on the uptake of SY dye onto AC; 10-40 mg/L, 35 min, 0.05-0.25 g, 600 rpm, pH 1 at room temperature

Fig. 4. Influence of contact time on the uptake of SY dye onto AC; 10-40 mg/L, 150 –250 μm , 0.05-0.25 g, 600 rpm, pH 1 at room temperature

Fig. 5. Influence of initial concentration and adsorbent dosage on the uptake of SY dye onto AC; 35 min, 150 –850 μm , 0.05-0.25 g, 600 rpm, pH 1 at room temperature

Fig. 6. Anticipated removal percentage plotted versus experimental data and the variation of the values forecasted by MGDH and MLR models from the actual values

1
2
3
4
5
6
7
8

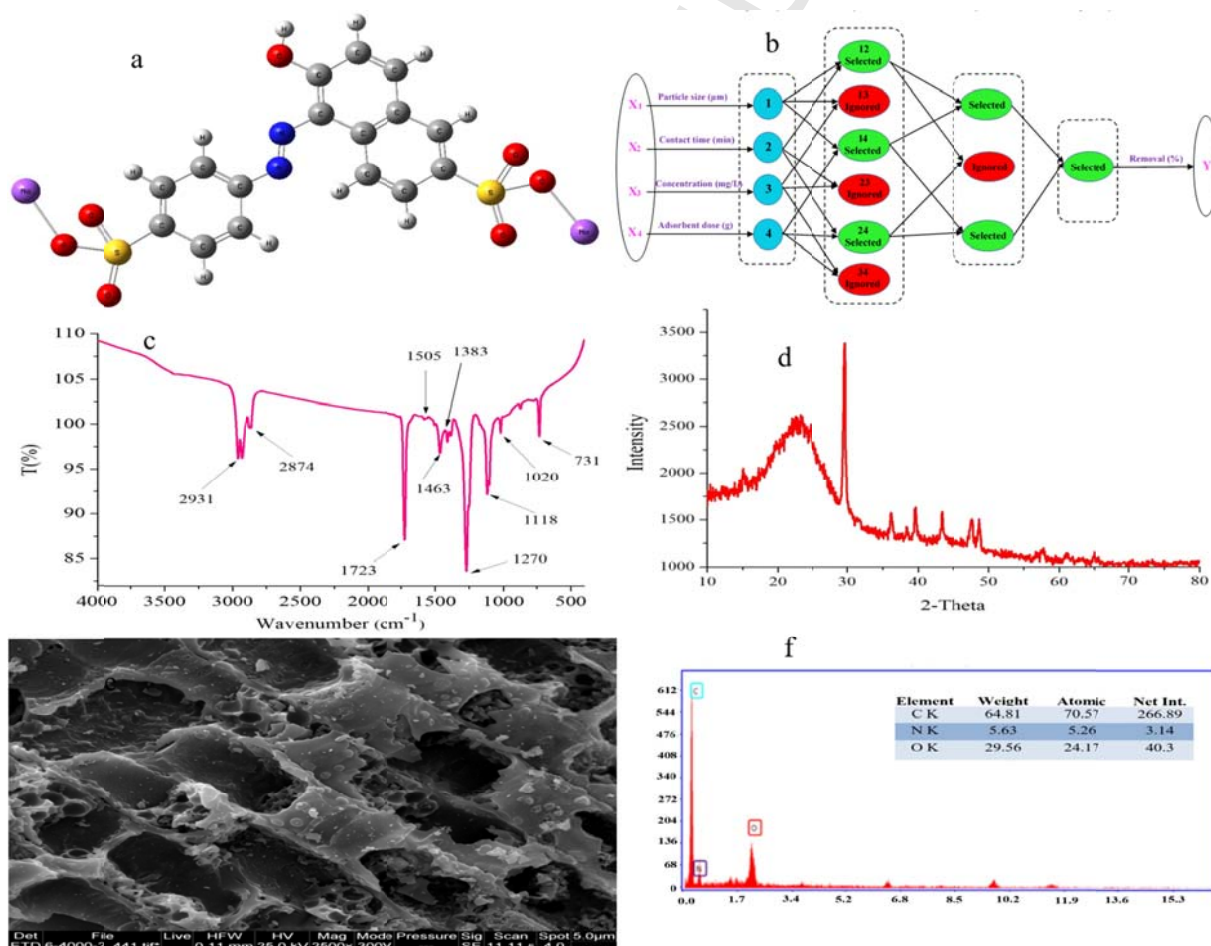
Table 1
Parameters of MGDH model and results of MSE and R²

Maximum Number of Neurons in a Layer	Maximum Number of Layers	Selection Pressure	Train Ratio	Train data		Test data	
				R ²	MSE	R ²	MSE
100	1	0.3	0.5	0.7603	31.5594	0.6655	38.1966
100	2	0.3	0.5	0.8312	22.2242	0.7771	25.4549
100	3	0.3	0.5	0.9639	4.7563	0.9537	5.2898
100	4	0.3	0.5	0.9653	4.5695	0.9557	5.0537
100	5	0.3	0.5	0.9696	4.0005	0.9602	4.5400
100	6	0.3	0.5	0.9752	3.2664	0.9663	3.8459
100	7	0.3	0.5	0.9772	3.0033	0.9656	3.9267
100	8	0.3	0.5	0.9755	3.2261	0.9519	5.4894
100	6	1.0	0.5	0.7565	32.0612	0.6658	38.1645
100	6	0.8	0.5	0.7595	31.6614	0.6826	36.2470
100	6	0.5	0.5	0.8329	22.0016	0.7791	25.2275
100	6	0.1	0.5	0.9748	3.3112	0.9670	3.7715
100	6	0.1	0.1	0.8806	15.7237	0.8601	15.9821
100	6	0.1	0.3	0.9597	5.3009	0.9518	5.4990
100	6	0.1	0.7	0.9785	2.8362	0.9702	3.4078
100	6	0.1	0.9	0.9762	3.1394	0.9653	3.9658
50	6	0.1	0.7	0.9715	3.7501	0.9589	4.6961
150	6	0.1	0.7	0.9770	3.0267	0.9627	4.2554

9
10
11
12
13

1
2
3
4
5

Fig. 1

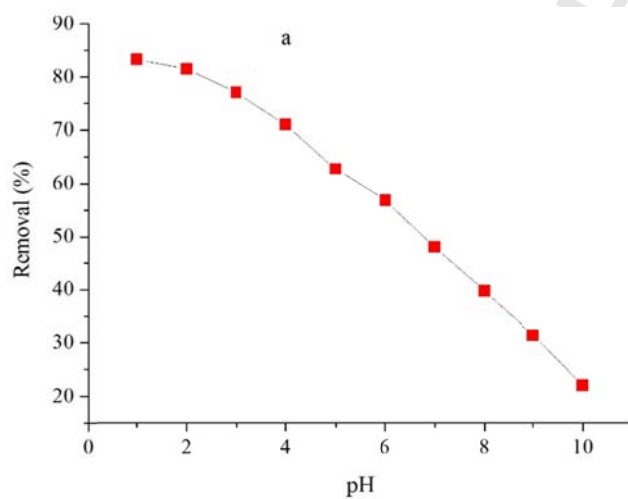
6
7
8

1

2

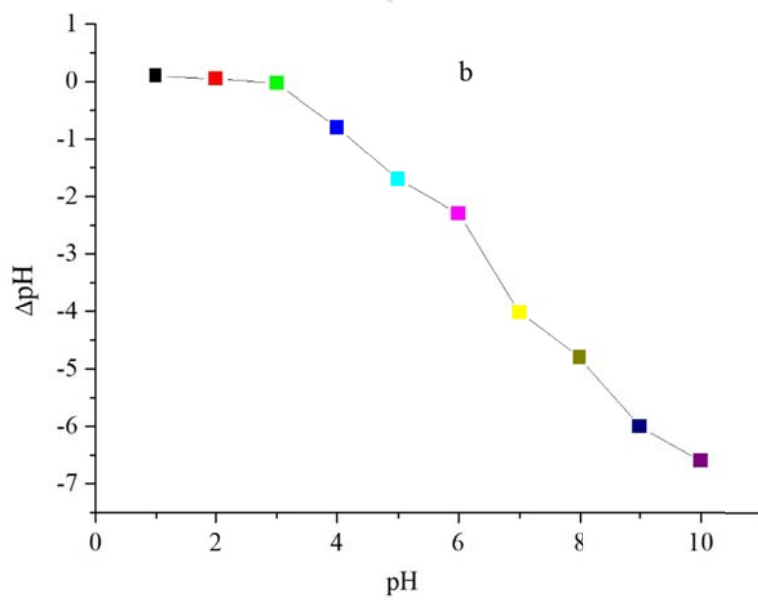
3

4 Fig. 2



5

6



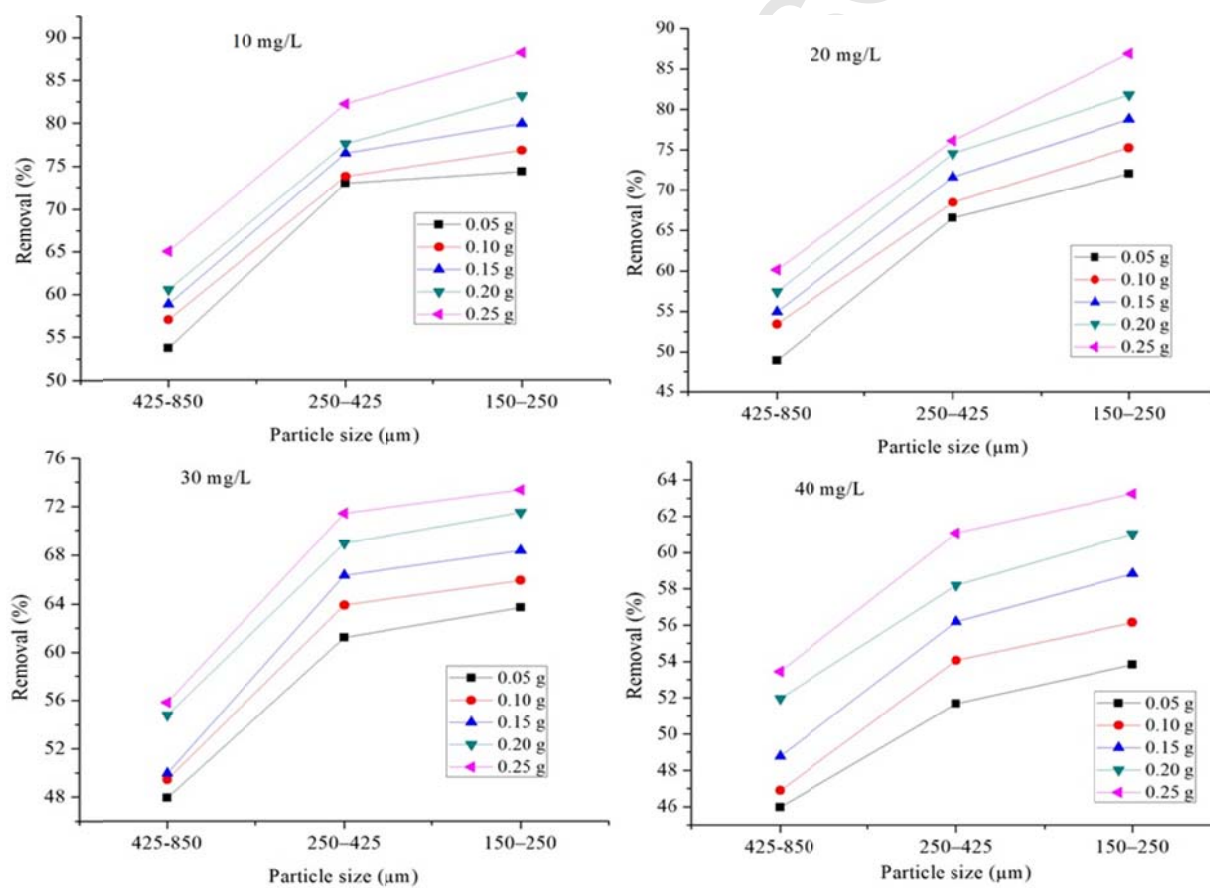
7

8

9

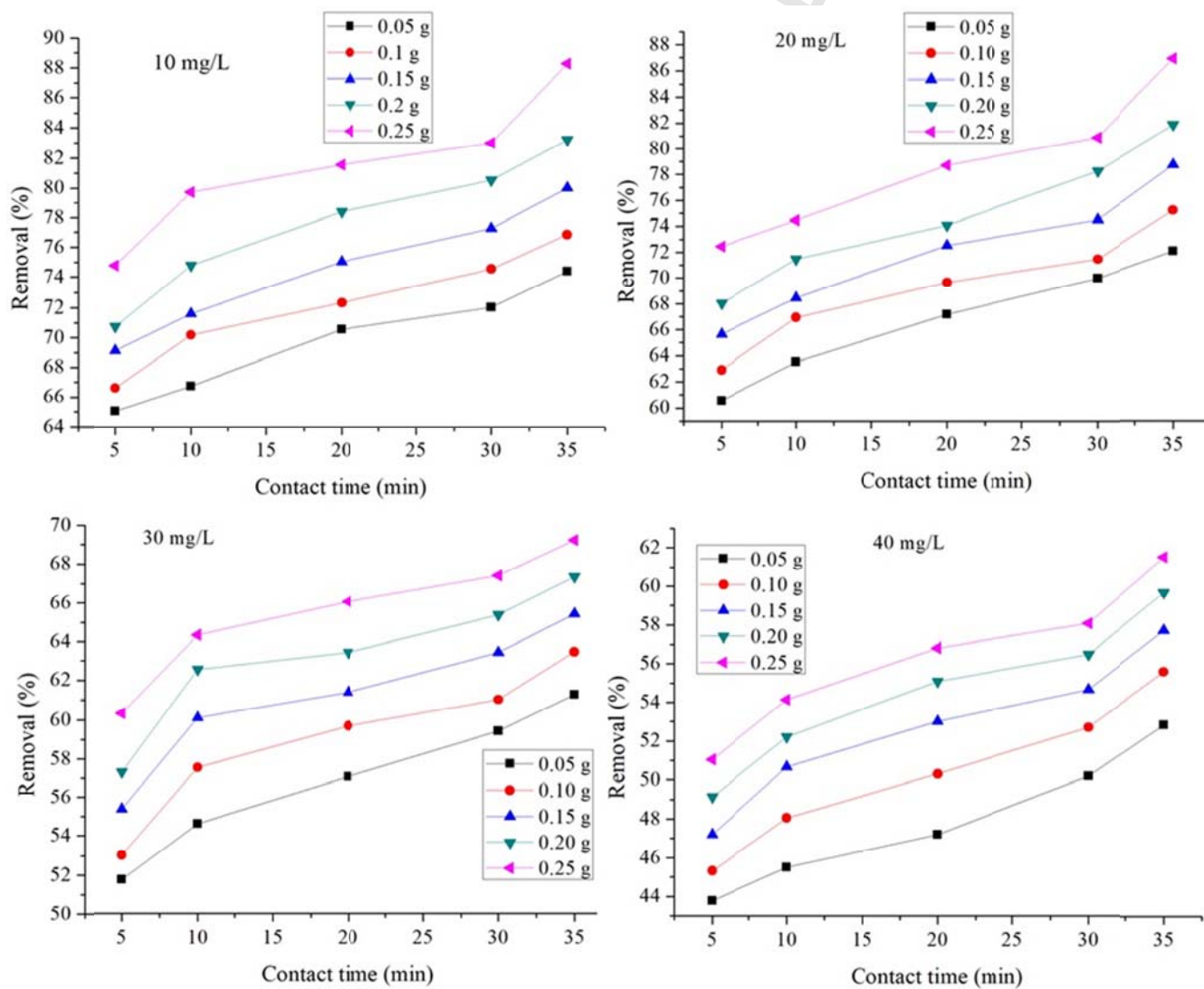
1
2
3
4
5
6

Fig.3

7
8
9
10
11
12
13

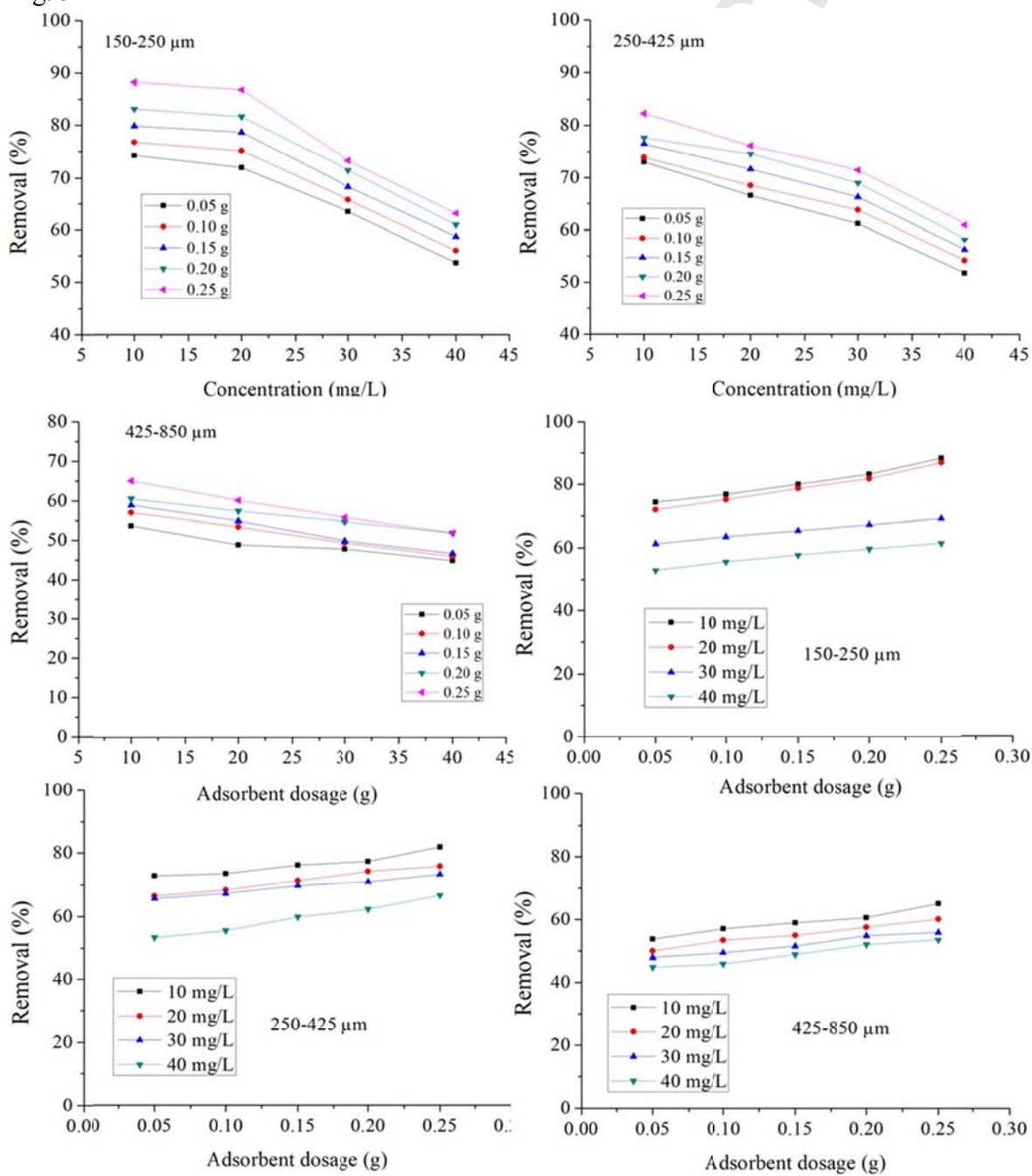
1
2
3
4
5

Fig. 4

6
7
8
9
10

1
2
3
4
5
6

Fig. 5

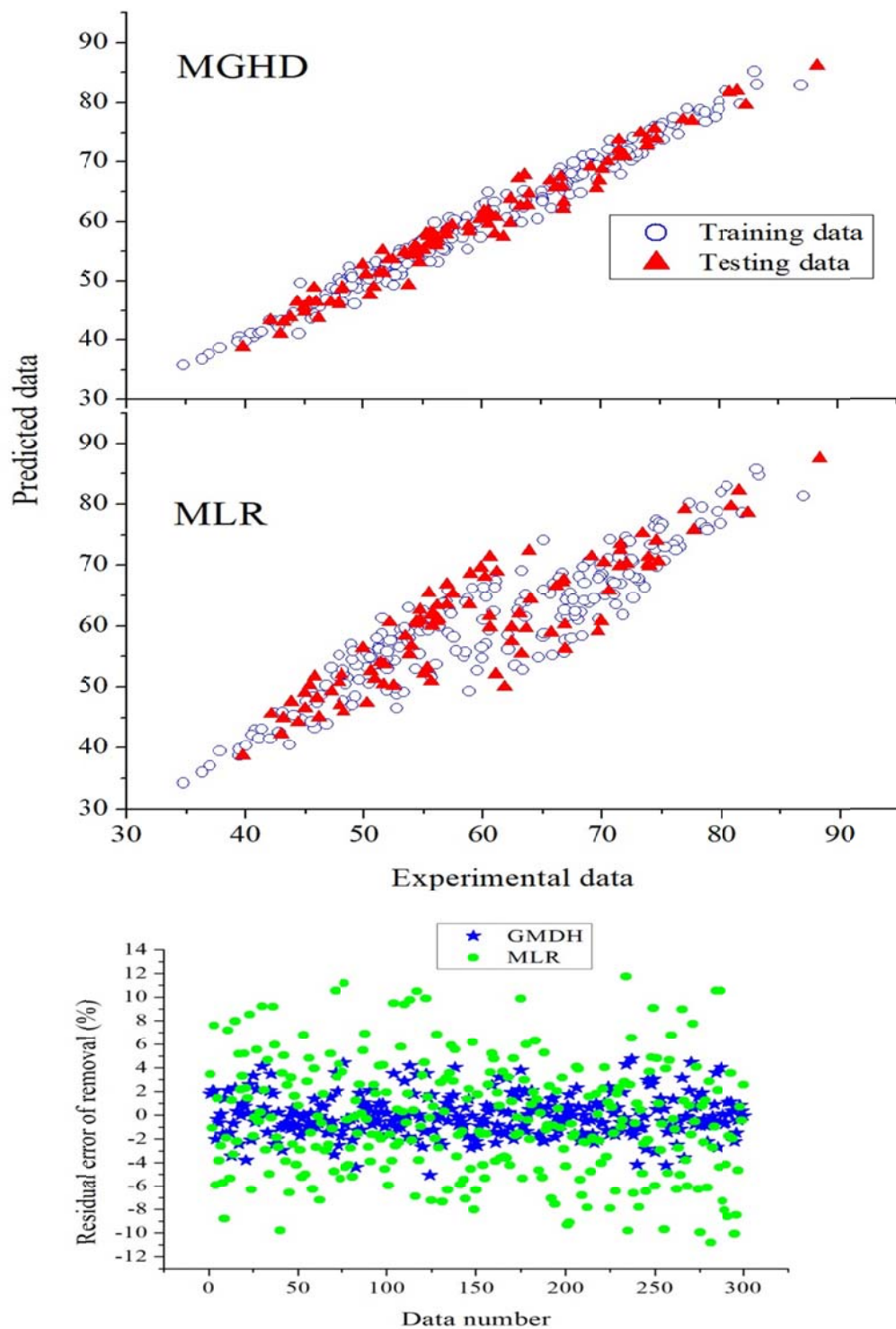


7

1

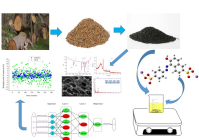
2

3 Fig. 6



4

ACCEPTED MANUSCRIPT



Highlights

1. AC from oak tree wood demonstrates efficient removal of Sunset Yellow dye from water.
2. Batch studies reveal optimum performance at pH 1 and contact time of 35 mins
3. Modeling reveals a better fit of experimental data with the Langmuir and pseudo-second order model
4. GMDH model shows better performance in forecasting removal of the dye.
5. Results reveal that soft computing model is a good tool for predicting adsorption performance